Published in final edited form as:
J Bone Miner Res. 2013 July ; 28(7): 1631–1640. doi:10.1002/jbmr.1894.

Periapical Disease and Bisphosphonates Induce Osteonecrosis of the Jaws in Mice

Ben Kang[1], **Simon Cheong**[1], **Thawinee Chaichanasakul**[1], **Olga Bezouglaia**[1], **Elisa Atti**[1], **Sarah M Dry**[2], **Flavia Q Pirih**[3], **Tara L. Aghaloo**[1,*], and **Sotirios Tetradis**[1,4,*]

[1]Division of Diagnostic and Surgical Sciences, UCLA School of Dentistry, Los Angeles, CA, 90095

[2]Department of Pathology and Laboratory Medicine, David Geffen School of Medicine at UCLA, Los Angeles, CA, 90095

[3]Division of Associated Specialties, UCLA School of Dentistry, Los Angeles, CA, 90095

[4]Molecular Biology Institute, UCLA, Los Angeles, CA, 90095

Abstract

Osteonecrosis of the jaw (ONJ) is a well-recognized complication of antiresorptive medications, such as bisphosphonates (BPs). Although ONJ is most common after tooth extractions in patients receiving high dose BPs, many patients do not experience oral trauma. Animal models utilizing tooth extractions and high BP doses recapitulate several clinical, radiographic and histologic findings of ONJ. We and others have reported on rat models of ONJ utilizing experimental dental disease in the absence of tooth extraction. These models emphasize the importance of dental infection/inflammation for ONJ development. Here, we extend our original report in the rat, and present a mouse model of ONJ in the presence of dental disease. Mice were injected with high dose zoledronic acid and pulpal exposure of mandibular molars was performed to induce periapical disease. After 8 weeks, quantitative and qualitative radiographic and histologic analyses of mouse mandibles were executed. Periapical lesions were larger in vehicle- vs. BP treated mice. Importantly, radiographic features resembling clinical ONJ, including thickening of the lamina dura, periosteal bone deposition and increased trabecular density, were seen in the drilled site of BP treated animals. Histologically, osteonecrosis, periosteal thickening, periosteal bone apposition, epithelial migration and bone exposure were present in the BP treated animals in the presence of periapical disease. No difference in TRAP+ cell numbers was observed, but round, detached, and removed from the bone surface cells were present in BP animals. Although 88% of the BP animals showed areas of osteonecrosis in the dental disease site, only 33% developed bone exposure, suggesting that osteonecrosis precedes bone exposure. Our data further emphasize the importance of dental disease in ONJ development, provide qualitative and quantitative measures of ONJ, and present a novel mouse ONJ model in the absence of tooth extraction that should be useful in further exploring ONJ pathophysiological mechanisms.

[*]Corresponding Authors: Sotirios Tetradis DDS, PhD, Diagnostic and Surgical Sciences, UCLA School of Dentistry, 10833 Le Conte Ave. CHS Rm. 53-068, Los Angeles, CA 90095-1668, Tel: (310) 825-5712, Fax: (310) 825-7232, stetradis@dentistry.ucla.edu, Tara Aghaloo DDS, MD, PhD, Diagnostic and Surgical Sciences, UCLA School of Dentistry, 10833 Le Conte Ave. CHS Rm. 53-009, Los Angeles, CA 90095-1668, Tel: (310)794-7070, Fax: (310)825-7232, taghaloo@dentistry.ucla.edu.

DISCLOSURES

Dr. Tetradis has served as a paid consultant for and has received grant support from Amgen Inc. All other authors state that they do not have any conflicts of interest.

Keywords

periapical disease; osteonecrosis of the jaws; bisphosphonate; mouse model; ONJ

INTRODUCTION

Bisphosphonates (BPs), stable analogs of natural occurring pyrophosphates, are potent inhibitors of osteoclastic-mediated bone resorption and have been used for over 30 years to treat postmenopausal osteoporosis, Paget's disease, hypercalcemia of malignancy and other metabolic bone diseases [1–4]. BPs rapidly localize to hydroxyapatite *in vivo* and are ingested by osteoclasts, altering the resorptive function and survival of these cells [5–7]. Zoledronate (ZA), delivered intravenously, and alendronate, administered orally, are examples of more potent nitrogen-containing BPs widely used in the management of cancer and skeletal disorders respectively [5, 8]. Mechanistically, nitrogen-containing BPs affect the mevalonate pathway by inhibiting the farnesyl diphosphate synthase, an enzyme important in the synthesis of farnesyl pyrophosphate for cholesterol biosynthesis [9]. This prevents the prenylation of small GTPase-signaling proteins such as Rho and Ras, which are important for osteoclast regulation of the cytoskeleton, intracellular vesicular transport and cell survival [10].

Although the use of BPs is beneficial for cancer and skeletal diseases treatments, BP related osteonecrosis of the jaws (ONJ) has been reported as a serious adverse effect of these drugs [11–13]. ONJ is most frequently observed after dental interventions such as tooth extraction, periodontal disease and in patients receiving corticosteroid treatment [11, 14, 15].

Despite having been described in the literature since 2004, ONJ etiology and pathophysiology remain largely unknown. Many hypotheses, including BP toxicity to oral epithelium, altered wound healing after tooth extraction, high turnover of the mandible and maxilla, oral biofilm formation, infection and inflammation, and suppression of angiogenesis and bone turnover have been proposed [16, 17]. Since the original ONJ reports, osteoclast inhibitors with different than BP pharmacologic action have been approved for treatment of bone malignancy and osteoporosis [18, 19]. Similar ONJ incidence has been observed with these medications [20–22], suggesting that inhibition of bone remodeling is central in the pathophysiology of the disease.

ONJ is a complex disease that involves the interaction of multiple tissues and cell types in response to local wound healing and/or infection under systemic pathologic conditions. As such, it would be difficult to replicate disease conditions *in vitro*. Animal models that capture several ONJ clinical, radiographic and histologic features have been developed in rats, mice and minipigs [23–31]. Most of these animal models involve tooth extraction in animals treated for prolonged periods with high-dose BP treatment, suggesting that BPs alter bone healing and lead to bone exposure. However, a significant fraction of ONJ diseases occurs in the absence of tooth extraction.

We recently published an animal model of ONJ utilizing rats that have undergone experimental periodontal disease of their first and second maxillary molars and were treated with high BP doses [24]. In these studies, no tooth extraction was performed. These findings paralleled studies in rats with diet-induced periodontitis [25] that similarly showed ONJ-like lesions in the presence of periodontal disease and BP treatment. These studies have collectively emphasized the importance of dental disease in ONJ pathophysiology. However, because they have been performed in rats, these animal models do not explore the full range of genetic and molecular biology tools available with mice.

Here, we have developed a mouse model of ONJ, without tooth extraction, but by applying experimental periapical disease in animals treated with high BP doses. Radiographic and histologic analysis revealed quantitative and qualitative differences in the alveolar structures of vehicle (veh) vs. BP treated animals. Importantly, the mice developed osteonecrotic lesions at high frequency that closely parallel radiographic and histologic features of ONJ in patients.

MATERIALS AND METHODS

Animal Care and Experimental Periapical Disease Induction

Animals and surgical procedures were handled according to guidelines of the UCLA Chancellor's Animal Research Committee. Thirty-five 4-month old C57BL/6J male mice (Jackson Laboratories, Bar Harbor, ME, USA) received intraperitoneal (IP) injections of veh (endotoxin free water) or 200 μg/kg zoledronic acid (BP group) three times per week for 1 week prior to periapical lesion induction. The dose of 200 μg/kg is approximately 3 fold higher than the oncologic zoledronic acid dose of 66 μg/kg [32], and in the range of experimental BP doses used in other animal models [27, 29]. We chose to use this higher dose to increase the incidence of ONJ in our animals, since there appears to be a dose-dependent effect of BPs on ONJ incidence in humans [33, 34].

Mice were anesthetized with isoflurane and mounted on a jaw retraction board. Pulpal exposure of the left first and second mandibular molars was performed utilizing a size 1/4 round bur, avoiding furcal perforation (Fig 1A, taken at sacrifice) as described [35, 36]. Exposed teeth were left open to the oral environment. Vehicle or ZA IP injections continued for an additional 7 weeks, following the same protocol of 200 μg/kg ZA at three times per week. We elected to inject the animals three times per week for the eight weeks of the experiment, to mimic the monthly injections in humans given the estimation that 17 days of a rodent life correspond to one human year [37]. Thus, the animals received a total of 24 ZA injections, which corresponds to 2 years of treatment for a cancer patient [38]. The mean time to onset of ONJ in patients treated with ZA is approximately 18 months [39].

At the end of the experiment, animals were sacrificed, mandibles were removed, placed in 4% paraformaldehyde for 48 hours and stored in 70% ethanol. Seventeen veh and 18 BP treated animals were utilized.

μCT Scanning

Mouse mandibles were imaged by μCT scanning (μCT SkyScan 1172; SkyScan, Kontich, Belgium) at 12 μm (0.012 mm) resolution, and volumetric data were converted to DICOM format and imported in the Dolphin Imaging software (Chatsworth, CA) to generate 3D and multiplanar reconstructed images [24]. To quantify the amount of periapical bone loss, the imaged volume was oriented so that the long axis of the distal root of the first molar (D1) was parallel to the coronal and sagittal planes. Then, the distance from the root apex to the periapical alveolar bone was measured at the distal root of the first and the mesial root of the second molars, for both the drilled and contralateral healthy sides.

To measure the width of the periodontal ligament (PDL) space and the thickness of the lamina dura at the furcation area of the first molars, a sagittal slice through the middle of the furcation area along the mesio-distal axis of the tooth was created. Three measurements at the middle of the mesial surface of the distal root, the tip of the furcation, and the middle of the distal surface of the mesial root were averaged to calculate the PDL space width and lamina dura thickness for each tooth.

To measure changes in the width of lingual bone thickness, the imaged volume was oriented such that the occlusal plane was parallel to the horizontal plane. The shortest distance from the lingual surface of the root to the lingual outline of the alveolar ridge was measured on an axial slice at the level of the apical third of the root for the distal root of the first molar and the mesial root of the second molar.

The alveolar bone, from the root apices to the alveolar crest, minus the roots and PDL space, was selected and the alveolar bone volume (BV), tissue volume (TV), and BV/TV were measured utilizing the CtAn software (Skyscan, Kontich, Belgium).

Histology and TRAP staining

After μCT scanning, mouse mandibular bones were decalcified in 14.5% ethylenediaminetetraacetic acid (EDTA) solution for three weeks. Samples were paraffin embedded and 5 μm-thick cross sections were made perpendicular to the long axis of the alveolar ridge along the distal root of the first molar. To quantify the number of empty osteocytic lacunae, area of osteonecrosis and periosteal thickness, hematoxylin and eosin (H&E)-stained slides were digitally scanned as described [24]. Using the ruler tool in ImageScope, the crestal 1-mm of the alveolar bone was marked. All measurements were performed in that area of the alveolar bone.

Within this area, the total number of empty and osteocytic lacunae and the osteonecrotic area(s), defined as a loss of more than five contiguous osteocytes with confluent areas of empty lacunae were measured. Furthermore, the total bone area and perimeter were assessed. To quantify periosteal bone thickness, the ruler tool was used to measure three greatest areas of both lingual and buccal periosteal thickness that were then averaged.

Tartrate-resistant acidic phosphatase (TRAP) positive cells were identified using the leukocyte acid phosphatase kit (Sigma-Aldrich, St. Louis, MO, USA) and counted under light microscope. All histology and digital imaging was performed at the Translational Pathology Core Laboratory (TPCL) at UCLA.

Statistics

Data among groups were analyzed using one-way analysis of variance (ANOVA). Data between groups were analyzed using Student’s t test.

RESULTS

Sagittal μCT sections through the apical area of the mandibular molars were created (Fig 1B). In healthy teeth of veh or BP treated animals, a continuous periodontal ligament (PDL) space and uniform lamina dura was observed. In drilled teeth of veh treated animals, widening of PDL space and loss of lamina dura, typical of periapical inflammation was observed. Interestingly, drilled teeth in BP treated animals showed a smaller increase in the PDL space widening and had retention of the lamina dura. A significant increase in the distance from the apex of the root to the alveolar bone (Fig 1C) was seen on the drilled side compared to the healthy side for both veh and BP treated animals (Fig. 1D). Importantly, BP treatment resulted in significantly less periapical bone loss for drilled teeth compared to veh treatment.

Bone changes extended along the roots to the furcation area of the drilled teeth. Fig. 2A shows sagittal sections through the furcation area of the 1st mandibular molars. In vehicle treated animals healthy teeth showed a thin PDL space along the root surface (indicated by the thick arrow), and a continuous uniform lamina dura (indicated by the thin arrow). Drilled teeth of veh treated animals showed an expansion of the PDL space and thinning of the

lamina dura. Healthy teeth of BP treated animals showed a normal PDL space. However, the lamina dura appeared thickened, compared to the healthy teeth of veh treated animals. Significantly, in BP treated animals, there was little widening of the PDL space and significant thickening of the lamina dura in the furcation area of drilled teeth. A statistically significant increase in PDL space and decrease in lamina dura thickness was seen in drilled teeth of veh treated animals (Fig. 2B, C and D). BP treatment caused a slight but statistically significant reduction in PDL space and a significant increase in lamina dura thickness in the furcation of healthy teeth. There was a small, statistically significant increase in PDL space at the furcation of drilled vs. healthy teeth in BP treated animals. However, this increase was significantly less compared to the PDL space increase in veh treated animals. Finally, drilled teeth in BP treated animals showed a statistically significant increase in lamina dura thickness compared to veh and BP treated healthy teeth.

The bone changes around the drilled teeth appeared to extend beyond the confines of the periodontal area to the adjacent alveolar bone (Fig. 3A). In vehicle treated animals, the alveolar bone around drilled teeth showed loss of trabecular integrity and osteolysis that extended to the mandibular cortices (Fig 3A, thick arrows). In contrast, the alveolar bone around drilled teeth of BP treated animals showed increased trabecular density and bone deposition on the periosteal surface of the buccal and lingual cortices (Fig. 3A, thin arrows). Seventeen (94%) BP treated animals and one (6%)veh treated animal, showed periosteal bone apposition (Table 1). The shortest distance from the bone perimeter to the root surface was measured for the lingual cortex (Fig. 3B). A significant decrease in bone thickness at the drilled teeth areas in veh treated animals was seen. BP treatment did not affect bone measurements. However, a significant increase in bone thickness was observed around drilled teeth in BP treated animals compared to healthy teeth of either veh or BP treated animals.

Then the BV, TV and BV/TV of the alveolar ridge were measured. No difference on TV among the various groups was seen (data not shown). Dental disease did not cause any change in BV or BV/TV in the veh treated animals. As expected, in the healthy site, BP treatment caused a significant increase of BV and BV/TV compared to veh treated mice. Importantly, dental disease caused an even greater increase in BV and BV/TV compared to the veh treated disease site and the healthy site of the BP treated animals (Fig 3D and E).

Histologic analysis showed that healthy teeth of both veh and BP treated animals had a normal PDL space and alveolar bone. Inflammatory infiltrate was observed in the apical areas of drilled teeth for both veh and BP treated animals (data not shown). Histologic examination of the periodontal molar areas revealed that healthy teeth of both veh and BP treated animals had normal periodontal structures, including marginal epithelium, crestal bone (Fig. 4A, A1, C and C1, red and aqua arrows) and periodontal ligament. Drilled teeth of both veh and treated animals showed inflammatory infiltrate at the gingival tissues (Fig. 4B, B1, D and D1, black arrows). Migration of marginal epithelium and reduction of the alveolar crest height was seen in the drilled teeth of veh treated animals (Fig. 4B and B1, red and aqua arrows). Although migration of marginal epithelium was also observed in the drilled teeth of BP treated animals (Fig. 4D and D1, red arrows) a smaller decrease in the alveolar crest height was present (Fig. 4D and D1, aqua arrows). As a result, the distance between the marginal epithelium and the alveolar crest was increased in the drilled vs. healthy site of veh treated animals, but was decreased in the drilled vs. healthy site of BP treated animals (Fig. 4B1 and D1, double arrows). Finally, areas of necrotic bone characterized by empty osteocytic lacunae and periosteal bone deposition were seen in the drilled site of 16 (88%) BP treated animals (Fig. 4D and D1, yellow and blue arrows respectively, and Table 1).

In six (33%) of the BP treated animals (Table 1), histologic assessment revealed epithelial migration below the level of the alveolar crest resulting in bone exposure (Fig. 5). At the lingual surface of the alveolar ridge, bone exposure (green arrows) and debris (red arrows) with epithelial migration (white arrows) along the necrotic bone (yellow arrow) to the level of periosteal bone deposition (blue arrows) were noted. At the buccal surface of the alveolar ridge, bone necrosis (yellow arrows) and periosteal bone deposition (blue arrows) but no bone exposure were seen. Inflammatory infiltrate (black arrows) was present throughout the alveolar ridge.

The thickness of the periosteum was measured on histologic sections at the lingual surface of the mandible. A significant increase in periosteal thickness was observed in the drilled vs. healthy side of the mouse mandibles. This increased thickness however, was more pronounced in the BP vs veh treated animals (Fig. 6A).

Then, the junctional epithelium to alveolar crest distance was measured on the lingual surface of the mandible in all animals (Fig. 6B). This distance significantly increased at the drilled site of the veh treated animals compared to the healthy site, suggesting increased resorption of the alveolar crest. In contrast, for the BP treatment animals, a significant decrease in the junctional epithelium to alveolar crest distance was observed, probably due to the apical migration of the junctional epithelium but reduced resorption of the alveolar crest.

To quantify the effect of the various treatments on osteocytes, the number of empty osteocytic lacunae of the alveolar ridge was measured (Fig. 6C). Interestingly, increased numbers of empty osteocytic lacunae were seen in the drilled vs. healthy site of veh treated animals, suggesting that dental disease causes osteocytic death. BP treatment in the healthy site also increased the number of empty osteocytic lacunae compared to the healthy site of veh treated animals. Importantly, the number of empty osteocytic lacunae in the drilled site of BP treated animals was significantly higher than the healthy site of the same animals and the drilled site of veh treated animals.

Evaluation of osteonecrotic areas (Fig. 6D) showed that osteonecrosis was present only in the drilled site of BP treated animals, while no osteonecrosis was seen in any of the other groups. These areas covered on average 25.5% of the alveolar bone area and measured 176,016 +/− 33,756 μm^2.

We further explored whether there was a difference in empty lacunae number outside the osteonecrotic areas. We thus, made the same measurements as in Fig. 6C, instead focusing on the areas of the alveolar bone outside osteonecrosis (Fig. 7B). For the healthy and drilled site of veh treated animals, and for the healthy site of BP treated animals, the same numbers of empty osteocytic lacunae as in Fig. 6C were seen. Surprisingly, the number of empty lacunae for the drilled site of BP treated animals was not different that the healthy site of the same animals or the drilled site of the veh treated animals (Fig. 7D).

During histologic evaluation, we observed that periosteal bone deposition was present adjacent to osteonecrotic areas in the drilled site of BP treated animals (Fig. 7A). We thus measured the % osteonecrotic area in a 50 μm zone next to the periosteal bone deposition (Fig. 7C). Indeed, a significantly higher osteonecrosis area was observed adjacent to periosteal bone deposits compared to the % osteonecrotic area for the overall alveolar bone (Fig. 7E).

Finally, TRAP assays (Fig. 8) showed a significant increase in the number of TRAP+ cells in the drilled vs. healthy site for both veh and BP treated animals. However, no difference was seen in the drilled site between veh and BP animals (Fig. 8A). Upon closer examination,

TRAP+ cells in the veh treated animals showed close attachment to the bone with an extended contact surface. In contrast, TRAP+ cells in the BP treated animals were round, detached, and at times removed from the bone surface (Fig. 8B).

DISCUSSION

Anti-resorptive therapies, are used for the management of bone diseases including hypercalcemia of malignancy, skeletal-related events and severe bone pain from primary or metastatic bone lesions, Paget's disease, osteoporosis and fibrous dysplasia [40, 41]. ONJ is a serious complication of potent antiresorptive medications such as BP and Denosumab, which directly affect osteoclast function and apoptosis or osteoclast formation and differentiation respectively. Elucidating ONJ pathophysiology and developing targeted therapies is of utmost importance in the management of the disease. To this end, we have focused our efforts on developing a clinically relevant rat, and now, mouse model of ONJ to characterize objective clinical, radiographic, and histologic signs of the disease.

Caries and periodontal disease, two of the most common infectious diseases [42], can compromise tooth structure and support, cause inflammation of the periodontal tissues and lead to tooth loss. In the uncompromised patient, the periapical alveolar bone or bony socket usually heal without difficulty after removal of the infectious/ inflammatory insult. The coordinated osteoclastic and osteoblastic activity is central in the healing process of the involved osseous structures. However, in patients taking intravenous BPs, the risk of abnormal healing after tooth extraction is apparent [15, 43, 44]. In fact, most reported ONJ cases occur after extraction, where extractions are usually performed for periodontal disease or deep caries extending to the periapical region [15, 43–48]. The decrease in ONJ incidence after dental preventive measures further supports the role of dental disease in ONJ pathophysiology [49, 50].

Based on these clinical observations, most animal models utilize tooth extractions and high-dose BP treatment, frequently in combination with dexamethasone or other chemotherapeutic agents, or metabolic deficiencies such as Vitamin D, to develop ONJ-like lesions in rats, mice or minipigs [23, 26–31]. In such models, delayed mucosal healing, ulceration, pseudoepitheliomatous hyperplasia, osteonecrosis, incomplete socket healing and bony sequestration have been described. Interestingly, others and we have reported on ONJ animal models in rats treated with high BP doses and undergone diet- or ligature-induced experimental periodontitis. These animals present clinical, radiographic and histologic features of ONJ, and recapitulate clinical ONJ in the absence of tooth extraction [24, 25, 51]. Here, we extend these studies and present a mouse ONJ model utilizing high-dose zoledronic acid and experimental periapical disease.

We utilized a well-established pulp exposure model of periapical disease that results in radiographically and histologically observed periapical lesions as early as 10 days after pulp exposure [35]. In this model, osteoclastic activity is central to alveolar bone resorption, and inhibition of osteoclastic activity results in decreased size of periapical lesions [52, 53]. In agreement with these findings, we observed that the size of periapical lesions at the apices of the molar roots was significantly smaller for the BP treated animals, as assessed by μCT imaging.

Importantly, μCT assessment of the alveolar bone revealed significant changes in bone morphology of the drilled site in BP treated animals that closely mimicked radiographic findings in ONJ patients. Diffuse osteosclerosis with increased trabecular density, thickening of cortical outlines with periosteal bone formation that is often extensive and thickening of the lamina dura have been described in conventional and CT radiographic

examinations of ONJ patients [54–58] and were present in the great majority (94%) of the BP treated animals around teeth with periapical disease. Histologic findings paralleled the radiographic observations, revealing that the thickness of the periosteum that lined the buccal and lingual cortices of the alveolar ridge increased substantially in the site with periapical disease compared to the healthy side for the BP treated animals. A more modest increase in periosteal thickness was seen in the diseased site of veh treated animals. We made similar observations in the ONJ rat model utilizing experimental periodontitis and high dose BP treatment [24].

Histologic examination revealed the presence of diffuse loss of osteocytes and empty osteocytic lacunae denoting alveolar bone osteonecrosis, in the diseased site of 16 (88%) BP treated animals. Interestingly, periapical disease or BP treatment alone caused a modest increase in the number of empty osteocytic lacunae that did not coalesce in osteonecrotic areas. When the number of empty osteocytic lacunae was measured in the alveolar bone outside the osteonecrotic areas, no statistical difference was detected among periapical disease, BP treatment or the combination of dental disease with BP treatment groups, which were all higher than the veh treated healthy group. This finding suggests that dental disease and BP treatment do not increase osteocytic death uniformly, but selectively to localized areas of the alveolar bone. Possible factors that might predispose such areas of the alveolus to osteonecrosis could include increased infection/inflammation or reduced vascularity.

Inhibition of osteoclastic activity appears to be central in ONJ pathophysiology, since clinical studies on patients treated with either BPs or Denosumab, a monoclonal antibody against RANKL, reveal a similar incidence of ONJ by both antiresorptive medications [20–22]. Osteoclasts with altered cell morphology, detached from the bone surface and undergoing apoptosis are seen in ONJ patients [55, 59] on BP treatment, as well as in ONJ animal models [25]. Similarly, we observed that although periapical disease increased TRAP + cell numbers in both vehicle and BP treated mice, BP treated animals showed round, and detached TRAP+ cells.

A noteworthy observation is that 75% of the alveolar bone in a 50 μm zone adjacent to the periosteal bone deposition was necrotic, suggesting that periosteal bone deposition developed adjacent to osteonecrotic areas. It would be important to establish in future experiments whether periosteal bone reaction develops prior to osteonecrosis or vice versa. This close association of periosteal bone reaction and osteonecrosis bears clinical significance, since our findings suggest that on radiographs of ONJ patients, osteonecrosis should be suspected not only in areas of sequestration but also in areas adjacent to periosteal bone apposition.

Although most of the mice presented with histologic osteonecrosis, only 33% showed exposed bone not covered by epithelium suggesting that bone exposure is not a prerequisite for bone necrosis. Similar observations have been reported in the rat ONJ models utilizing experimental periodontis [24, 25], as well as with ONJ models utilizing tooth extraction [27]. These findings could have two potential implications for the clinical setting. First, in cancer patients, alveolar bone necrosis might be present around teeth with extensive periodontal or periapical disease. Extraction of such teeth would further exacerbate tissue injury and complicate healing. Second, the mice with histologic and radiographic features of ONJ but without frank bone exposure appear to resemble patients on BP treatment that present with ONJ-like radiographic or clinical symptoms but without orally exposed bone [60–63]. The original ONJ staging system has recently been changed to add stage 0 disease to include these patients [44].

Since our animal model did not include tooth extraction there was no experimental violation of mucosal integrity. Migration of the marginal epithelium on the diseased site of both veh and BP treated animals was observed. However, in the veh treated animals concurrent bone resorption resulted in increased epithelial-bone crest distance. In contrast, BP treated animals showed a significant reduction of the epithelial-bone crest distance. Importantly, in the animals with bone exposure the migrating epithelium bypassed the osteonecrotic bone to extend to the area of the vital periosteal bone apposition, thus resulting in bone exposure.

In our studies, similar to other published reports [27, 29], we utilized high doses of ZA, a nitrogen-containing potent BP to induce ONJ-like lesions in the jaws of mice that closely mimic the clinical, radiographic and histologic features of human ONJ. These injection doses are approximately 3 fold higher than the ZA injection doses used in patients with bone malignancy [32]. Although these animal models appear to capture the basic ONJ pathophysiologic mechanisms, interpretation of findings should consider the possibility of additional cell or tissue effects by the high ZA doses. Furthermore, these higher ZA doses most probably underlie the higher incidence of osteonecrosis observed in our studies, compared with published patient data [44, 64]. Future studies with pharmacologic doses similar to clinical regimens will expand utilization of this animal model and provide a more accurate assessment of ONJ incidence and severity.

In summary, we have created a mouse model with significant clinical, radiographic and histologic resemblance to ONJ in patients. This model enhances existing mouse models utilizing tooth extraction, as it addresses a subset of ONJ occurrence in the absence of traumatic interventions. Furthermore, this mouse model complements other rat ONJ models utilizing experimental dental disease, and provides the benefits of working in a system with rich genetic and molecular tools that should assist studies of ONJ pathophysiology and targeted therapies.

Acknowledgments

This work was supported by NIH/NIDCR DE019465 and minority supplement DE 019465- S1.

Authors' roles: All authors participated in the design, execution and analyses of the studies. BK, SC, TA and ST drafted the manuscript. All authors made revisions to the manuscript and approved the final version.

REFERENCES

1. Allen MR. Bisphosphonates and osteonecrosis of the jaw: moving from the bedside to the bench. Cells Tissues Organs. 2009; 189:289–294. [PubMed: 18698128]
2. Russell RG. Bisphosphonates: the first 40 years. Bone. 2011; 49:2–19. [PubMed: 21555003]
3. Russell RG, Watts NB, Ebetino FH, Rogers MJ. Mechanisms of action of bisphosphonates: similarities and differences and their potential influence on clinical efficacy. Osteoporos Int. 2008; 19:733–759. [PubMed: 18214569]
4. Roelofs AJ, Thompson K, Gordon S, Rogers MJ. Molecular mechanisms of action of bisphosphonates: current status. Clin Cancer Res. 2006; 12:6222s–6230s. [PubMed: 17062705]
5. Russell RG, Rogers MJ. Bisphosphonates: from the laboratory to the clinic and back again. Bone. 1999; 25:97–106. [PubMed: 10423031]
6. Sato M, Grasser W, Endo N, Akins R, Simmons H, Thompson DD, Golub E, Rodan GA. Bisphosphonate action. Alendronate localization in rat bone and effects on osteoclast ultrastructure. J Clin Invest. 1991; 88:2095–2105. [PubMed: 1661297]
7. Thompson K, Rogers MJ, Coxon FP, Crockett JC. Cytosolic entry of bisphosphonate drugs requires acidification of vesicles after fluid-phase endocytosis. Mol Pharmacol. 2006; 69:1624–1632. [PubMed: 16501031]

8. Winter MC, Holen I, Coleman RE. Exploring the anti-tumour activity of bisphosphonates in early breast cancer. Cancer Treat Rev. 2008; 34:453–475. [PubMed: 18423992]
9. Luckman SP, Hughes DE, Coxon FP, Graham R, Russell G, Rogers MJ. Nitrogen-containing bisphosphonates inhibit the mevalonate pathway and prevent post-translational prenylation of GTP-binding proteins, including Ras. J Bone Miner Res. 1998; 13:581–589. [PubMed: 9556058]
10. Kimmel DB. Mechanism of action, pharmacokinetic and pharmacodynamic profile, and clinical applications of nitrogen-containing bisphosphonates. J Dent Res. 2007; 86:1022–1033. [PubMed: 17959891]
11. Migliorati CA, Schubert MM, Peterson DE, Seneda LM. Bisphosphonate-associated osteonecrosis of mandibular and maxillary bone: an emerging oral complication of supportive cancer therapy. Cancer. 2005; 104:83–93. [PubMed: 15929121]
12. Christodoulou C, Pervena A, Klouvas G, Galani E, Falagas ME, Tsakalos G, Visvikis A, Nikolakopoulou A, Acholos V, Karapanagiotidis G, Batziou E, Skarlos DV. Combination of bisphosphonates and antiangiogenic factors induces osteonecrosis of the jaw more frequently than bisphosphonates alone. Oncology. 2009; 76:209–211. [PubMed: 19212145]
13. Ruggiero SL, Mehrotra B, Rosenberg TJ, Engroff SL. Osteonecrosis of the jaws associated with the use of bisphosphonates: a review of 63 cases. J Oral Maxillofac Surg. 2004; 62:527–534. [PubMed: 15122554]
14. Marx RE. Pamidronate (Aredia) and zoledronate (Zometa) induced avascular necrosis of the jaws: a growing epidemic. J Oral Maxillofac Surg. 2003; 61:1115–1117. [PubMed: 12966493]
15. Marx RE, Sawatari Y, Fortin M, Broumand V. Bisphosphonate-induced exposed bone (osteonecrosis/osteopetrosis) of the jaws: risk factors, recognition, prevention, and treatment. J Oral Maxillofac Surg. 2005; 63:1567–1575. [PubMed: 16243172]
16. Landesberg R, Woo V, Cremers S, Cozin M, Marolt D, Vunjak-Novakovic G, Kousteni S, Raghavan S. Potential pathophysiological mechanisms in osteonecrosis of the jaw. Ann N Y Acad Sci. 2011; 1218:62–79. [PubMed: 21291478]
17. Yamashita J, McCauley LK. Antiresorptives and osteonecrosis of the jaw. J Evid Based Dent Pract. 2012; 12:233–247. [PubMed: 23040351]
18. Goessl C, Katz L, Dougall WC, Kostenuik PJ, Zoog HB, Braun A, Dansey R, Wagman RB. The development of denosumab for the treatment of diseases of bone loss and cancer-induced bone destruction. Ann N Y Acad Sci. 2012; 1263:29–40. [PubMed: 22831177]
19. Sinningen K, Tsourdi E, Rauner M, Rachner TD, Hamann C, Hofbauer LC. Skeletal and extraskeletal actions of denosumab. Endocrine. 2012; 42:52–62. [PubMed: 22581255]
20. Lipton A, Fizazi K, Stopeck AT, Henry DH, Brown JE, Yardley DA, Richardson GE, Siena S, Maroto P, Clemens M, Bilynskyy B, Charu V, Beuzeboc P, Rader M, Viniegra M, Saad F, Ke C, Braun A, Jun S. Superiority of denosumab to zoledronic acid for prevention of skeletal-related events: a combined analysis of 3 pivotal, randomised, phase 3 trials. Eur J Cancer. 2012; 48:3082–3092. [PubMed: 22975218]
21. Peddi P, Lopez-Olivo MA, Pratt GF, Suarez-Almazor ME. Denosumab in patients with cancer and skeletal metastases: A systematic review and meta-analysis. Cancer Treat Rev. 2013; 39:97–104. [PubMed: 22898302]
22. Scagliotti GV, Hirsh V, Siena S, Henry DH, Woll PJ, Manegold C, Solal-Celigny P, Rodriguez G, Krzakowski M, Mehta ND, Lipton L, Garcia-Saenz JA, Pereira JR, Prabhash K, Ciuleanu TE, Kanarev V, Wang H, Balakumaran A, Jacobs I. Overall Survival Improvement in Patients with Lung Cancer and Bone Metastases Treated with Denosumab Versus Zoledronic Acid: Subgroup Analysis from a Randomized Phase 3 Study. J Thorac Oncol. 2012; 7:1823–1829. [PubMed: 23154554]
23. Abtahi J, Agholme F, Sandberg O, Aspenberg P. Bisphosphonate-induced osteonecrosis of the jaw in a rat model arises first after the bone has become exposed. No primary necrosis in unexposed bone. J Oral Pathol Med. 2012; 41:494–499. [PubMed: 22268631]
24. Aghaloo TL, Kang B, Sung EC, Shoff M, Ronconi M, Gotcher JE, Bezouglaia O, Dry SM, Tetradis S. Periodontal disease and bisphosphonates induce osteonecrosis of the jaws in the rat. J Bone Miner Res. 2011; 26:1871–1882. [PubMed: 21351151]

25. Aguirre JI, Akhter MP, Kimmel DB, Pingel JE, Williams A, Jorgensen M, Kesavalu L, Wronski TJ. Oncologic doses of zoledronic acid induce osteonecrosis of the jaw-like lesions in rice rats (Oryzomys palustris) with periodontitis. J Bone Miner Res. 2012; 27:2130–2143. [PubMed: 22623376]
26. Ali-Erdem M, Burak-Cankaya A, Cemil-Isler S, Demircan S, Soluk M, Kasapoglu C, Korhan-Oral C. Extraction socket healing in rats treated with bisphosphonate: animal model for bisphosphonate related osteonecrosis of jaws in multiple myeloma patients. Med Oral Patol Oral Cir Bucal. 2011; 16:e879–e883. [PubMed: 21743422]
27. Bi Y, Gao Y, Ehirchiou D, Cao C, Kikuiri T, Le A, Shi S, Zhang L. Bisphosphonates cause osteonecrosis of the jaw-like disease in mice. Am J Pathol. 2010; 177:280–290. [PubMed: 20472893]
28. Lopez-Jornet P, Camacho-Alonso F, Molina-Minano F, Gomez-Garcia F, Vicente-Ortega V. An experimental study of bisphosphonate-induced jaws osteonecrosis in Sprague-Dawley rats. J Oral Pathol Med. 2010; 39:697–702. [PubMed: 20819131]
29. Kikuiri T, Kim I, Yamaza T, Akiyama K, Zhang Q, Li Y, Chen C, Chen W, Wang S, Le AD, Shi S. Cell-based immunotherapy with mesenchymal stem cells cures bisphosphonate-related osteonecrosis of the jaw-like disease in mice. J Bone Miner Res. 2010; 25:1668–1679. [PubMed: 20200952]
30. Sonis ST, Watkins BA, Lyng GD, Lerman MA, Anderson KC. Bony changes in the jaws of rats treated with zoledronic acid and dexamethasone before dental extractions mimic bisphosphonate-related osteonecrosis in cancer patients. Oral Oncol. 2009; 45:164–172. [PubMed: 18715819]
31. Pautke C, Kreutzer K, Weitz J, Knodler M, Munzel D, Wexel G, Otto S, Hapfelmeier A, Sturzenbaum S, Tischer T. Bisphosphonate related osteonecrosis of the jaw: A minipig large animal model. Bone. 2012; 51:592–599. [PubMed: 22575441]
32. Kyle RA, Yee GC, Somerfield MR, Flynn PJ, Halabi S, Jagannath S, Orlowski RZ, Roodman DG, Twilde P, Anderson K. American Society of Clinical Oncology 2007 clinical practice guideline update on the role of bisphosphonates in multiple myeloma. J Clin Oncol. 2007; 25:2464–2472. [PubMed: 17515569]
33. Vahtsevanos K, Kyrgidis A, Verrou E, Katodritou E, Triaridis S, Andreadis CG, Boukovinas I, Koloutsos GE, Teleioudis Z, Kitikidou K, Paraskevopoulos P, Zervas K, Antoniades K. Longitudinal cohort study of risk factors in cancer patients of bisphosphonate-related osteonecrosis of the jaw. J Clin Oncol. 2009; 27:5356–5362. [PubMed: 19805682]
34. Fehm T, Beck V, Banys M, Lipp HP, Hairass M, Reinert S, Solomayer EF, Wallwiener D, Krimmel M. Bisphosphonate-induced osteonecrosis of the jaw (ONJ): Incidence and risk factors in patients with breast cancer and gynecological malignancies. Gynecol Oncol. 2009; 112:605–609. [PubMed: 19136147]
35. Wang CY, Stashenko P. Kinetics of bone-resorbing activity in developing periapical lesions. J Dent Res. 1991; 70:1362–1366. [PubMed: 1939830]
36. Sasaki H, Hou L, Belani A, Wang CY, Uchiyama T, Muller R, Stashenko P. IL-10, but not IL-4, suppresses infection-stimulated bone resorption in vivo. J Immunol. 2000; 165:3626–3630. [PubMed: 11034365]
37. Quinn R. Comparing rat's to human's age: how old is my rat in people years? Nutrition. 2005; 21:775–777. [PubMed: 15925305]
38. Ibrahim A, Scher N, Williams G, Sridhara R, Li N, Chen G, Leighton J, Booth B, Gobburu JV, Rahman A, Hsieh Y, Wood R, Vause D, Pazdur R. Approval summary for zoledronic acid for treatment of multiple myeloma and cancer bone metastases. Clin Cancer Res. 2003; 9:2394–2399. [PubMed: 12855610]
39. Maerevoet M, Martin C, Duck L. Osteonecrosis of the jaw and bisphosphonates. N Engl J Med. 2005; 353:99–102. discussion 199-102. [PubMed: 16003838]
40. Coleman RE, Major P, Lipton A, Brown JE, Lee KA, Smith M, Saad F, Zheng M, Hei YJ, Seaman J, Cook R. Predictive value of bone resorption and formation markers in cancer patients with bone metastases receiving the bisphosphonate zoledronic acid. J Clin Oncol. 2005; 23:4925–4935. [PubMed: 15983391]

41. Stewart AF. Clinical practice. Hypercalcemia associated with cancer. N Engl J Med. 2005; 352:373–379. [PubMed: 15673803]
42. Evans CA, Kleinman DV. The Surgeon General's report on America's oral health: opportunities for the dental profession. J Am Dent Assoc. 2000; 131:1721–1728. [PubMed: 11143736]
43. Andriani A, Petrucci MT, Caravita T, Montanaro M, Villiva N, Levi A, Siniscalchi A, Bongarzoni V, Pisani F, De Muro M, Coppetelli U, Avvisati G, Zullo A, Agrillo A, Gaglioti D. Evolution of bisphosphonate-related osteonecrosis of the jaw in patients with multiple myeloma and Waldenstrom's macroglobulinemia: a retrospective multicentric study. Blood Cancer J. 2012; 2:e62. [PubMed: 22829257]
44. Ruggiero SL, Dodson TB, Assael LA, Landesberg R, Marx RE, Mehrotra B. American Association of Oral and Maxillofacial Surgeons position paper on bisphosphonate-related osteonecrosis of the jaws--2009 update. J Oral Maxillofac Surg. 2009; 67:2–12. [PubMed: 19371809]
45. Bilezikian JP. Osteonecrosis of the jaw--do bisphosphonates pose a risk? N Engl J Med. 2006; 355:2278–2281. [PubMed: 17135582]
46. Ficarra G, Beninati F, Rubino I, Vannucchi A, Longo G, Tonelli P, Pini Prato G. Osteonecrosis of the jaws in periodontal patients with a history of bisphosphonates treatment. J Clin Periodontol. 2005; 32:1123–1128. [PubMed: 16212571]
47. Lo JC, O'Ryan FS, Gordon NP, Yang J, Hui RL, Martin D, Hutchinson M, Lathon PV, Sanchez G, Silver P, Chandra M, McCloskey CA, Staffa JA, Willy M, Selby JV, Go AS. Prevalence of osteonecrosis of the jaw in patients with oral bisphosphonate exposure. J Oral Maxillofac Surg. 2010; 68:243–253. [PubMed: 19772941]
48. Mavrokokki T, Cheng A, Stein B, Goss A. Nature and frequency of bisphosphonate-associated osteonecrosis of the jaws in Australia. J Oral Maxillofac Surg. 2007; 65:415–423. [PubMed: 17307586]
49. Dimopoulos MA, Kastritis E, Anagnostopoulos A, Melakopoulos I, Gika D, Moulopoulos LA, Bamia C, Terpos E, Tsionos K, Bamias A. Osteonecrosis of the jaw in patients with multiple myeloma treated with bisphosphonates: evidence of increased risk after treatment with zoledronic acid. Haematologica. 2006; 91:968–971. [PubMed: 16757414]
50. Ripamonti CI, Maniezzo M, Campa T, Fagnoni E, Brunelli C, Saibene G, Bareggi C, Ascani L, Cislaghi E. Decreased occurrence of osteonecrosis of the jaw after implementation of dental preventive measures in solid tumour patients with bone metastases treated with bisphosphonates. The experience of the National Cancer Institute of Milan. Ann Oncol. 2009; 20:137–145. [PubMed: 18647964]
51. Gotcher JE, Jee WS. The progress of the periodontal syndrome in the rice cat. II. The effects of a diphosphonate on the periodontium. J Periodontal Res. 1981; 16:441–455. [PubMed: 6459441]
52. Gao B, Chen W, Hao L, Zhu G, Feng S, Ci H, Zhou X, Stashenko P, Li YP. Inhibiting Periapical Lesions through AAV-RNAi Silencing of Cathepsin K. J Dent Res. 2012
53. Wang CY, Tani-Ishii N, Stashenko P. Bone-resorptive cytokine gene expression in periapical lesions in the rat. Oral Microbiol Immunol. 1997; 12:65–71. [PubMed: 9227128]
54. Arce K, Assael LA, Weissman JL, Markiewicz MR. Imaging findings in bisphosphonate-related osteonecrosis of jaws. J Oral Maxillofac Surg. 2009; 67:75–84. [PubMed: 19371818]
55. Bedogni A, Blandamura S, Lokmic Z, Palumbo C, Ragazzo M, Ferrari F, Tregnaghi A, Pietrogrande F, Procopio O, Saia G, Ferretti M, Bedogni G, Chiarini L, Ferronato G, Ninfo V, Lo Russo L, Lo Muzio L, Nocini PF. Bisphosphonate-associated jawbone osteonecrosis: a correlation between imaging techniques and histopathology. Oral Surg Oral Med Oral Pathol Oral Radiol Endod. 2008; 105:358–364. [PubMed: 18280968]
56. Bianchi SD, Scoletta M, Cassione FB, Migliaretti G, Mozzati M. Computerized tomographic findings in bisphosphonate-associated osteonecrosis of the jaw in patients with cancer. Oral Surg Oral Med Oral Pathol Oral Radiol Endod. 2007; 104:249–258. [PubMed: 17560140]
57. Elad S, Gomori MJ, Ben-Ami N, Friedlander-Barenboim S, Regev E, Lazarovici TS, Yarom N. Bisphosphonate-related osteonecrosis of the jaw: clinical correlations with computerized tomography presentation. Clin Oral Investig. 2010; 14:43–50.

58. Phal PM, Myall RW, Assael LA, Weissman JL. Imaging findings of bisphosphonate-associated osteonecrosis of the jaws. AJNR Am J Neuroradiol. 2007; 28:1139–1145. [PubMed: 17569974]

59. Cho YA, Yoon HJ, Lee JI, Hong SP, Hong SD. Histopathological features of bisphosphonate-associated osteonecrosis: findings in patients treated with partial mandibulectomies. Oral Surg Oral Med Oral Pathol Oral Radiol. 2012; 114:785–791. [PubMed: 23159117]

60. Fedele S, Porter SR, D'Aiuto F, Aljohani S, Vescovi P, Manfredi M, Arduino PG, Broccoletti R, Musciotto A, Di Fede O, Lazarovici TS, Campisi G, Yarom N. Nonexposed variant of bisphosphonate-associated osteonecrosis of the jaw: a case series. Am J Med. 2010; 123:1060–1064. [PubMed: 20851366]

61. Hutchinson M, O'Ryan F, Chavez V, Lathon PV, Sanchez G, Hatcher DC, Indresano AT, Lo JC. Radiographic findings in bisphosphonate-treated patients with stage 0 disease in the absence of bone exposure. J Oral Maxillofac Surg. 2010; 68:2232–2240. [PubMed: 20728032]

62. Junquera L, Gallego L. Nonexposed bisphosphonate-related osteonecrosis of the jaws: another clinical variant? J Oral Maxillofac Surg. 2008; 66:1516–1517. [PubMed: 18571043]

63. Patel S, Choyee S, Uyanne J, Nguyen AL, Lee P, Sedghizadeh PP, Kumar SK, Lytle J, Shi S, Le AD. Non-exposed bisphosphonate-related osteonecrosis of the jaw: a critical assessment of current definition, staging, and treatment guidelines. Oral Dis. 2012; 18:625–632. [PubMed: 22420684]

64. Khosla S, Burr D, Cauley J, Dempster DW, Ebeling PR, Felsenberg D, Gagel RF, Gilsanz V, Guise T, Koka S, McCauley LK, McGowan J, McKee MD, Mohla S, Pendrys DG, Raisz LG, Ruggiero SL, Shafer DM, Shum L, Silverman SL, Van Poznak CH, Watts N, Woo SB, Shane E. Bisphosphonate-associated osteonecrosis of the jaw: report of a task force of the American Society for Bone and Mineral Research. J Bone Miner Res. 2007; 22:1479–1491. [PubMed: 17663640]

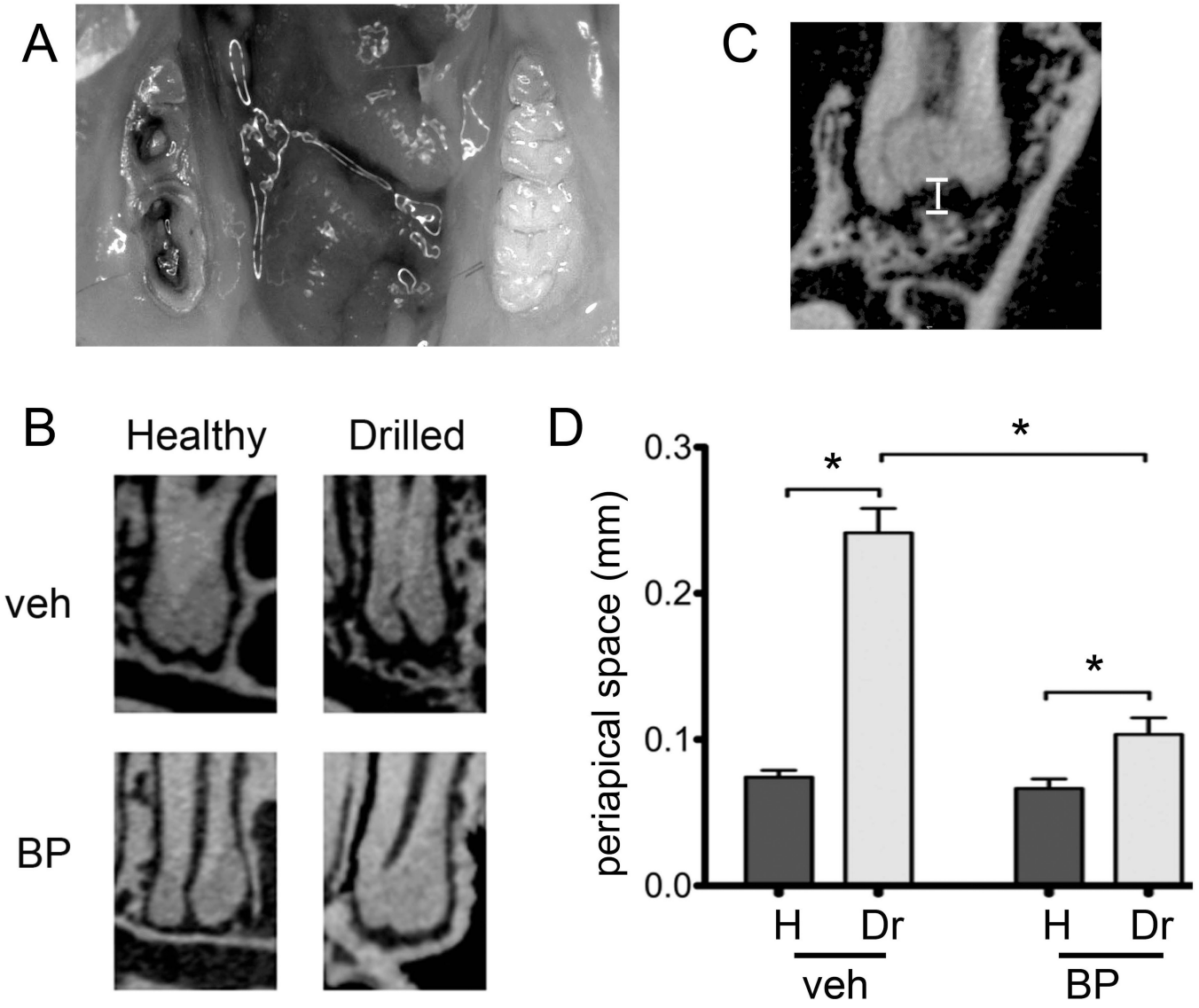

Figure 1.

Experimental periapical disease model. A) The crowns of the first and second molars were drilled to create pulp exposure and cause periapical disease in veh or BP treated animals. B) Representative μCT images of the periapical area of the first molar distal root of healthy and drilled sites in veh or BP treated animals are shown. C) To quantify periapical bone loss, the periapical space was measured as the distance from the root apex to the periapical alveolar bone. D) Periapical space at the distal root of the first molar (D1). * statistically significantly different, $p<0.01$.

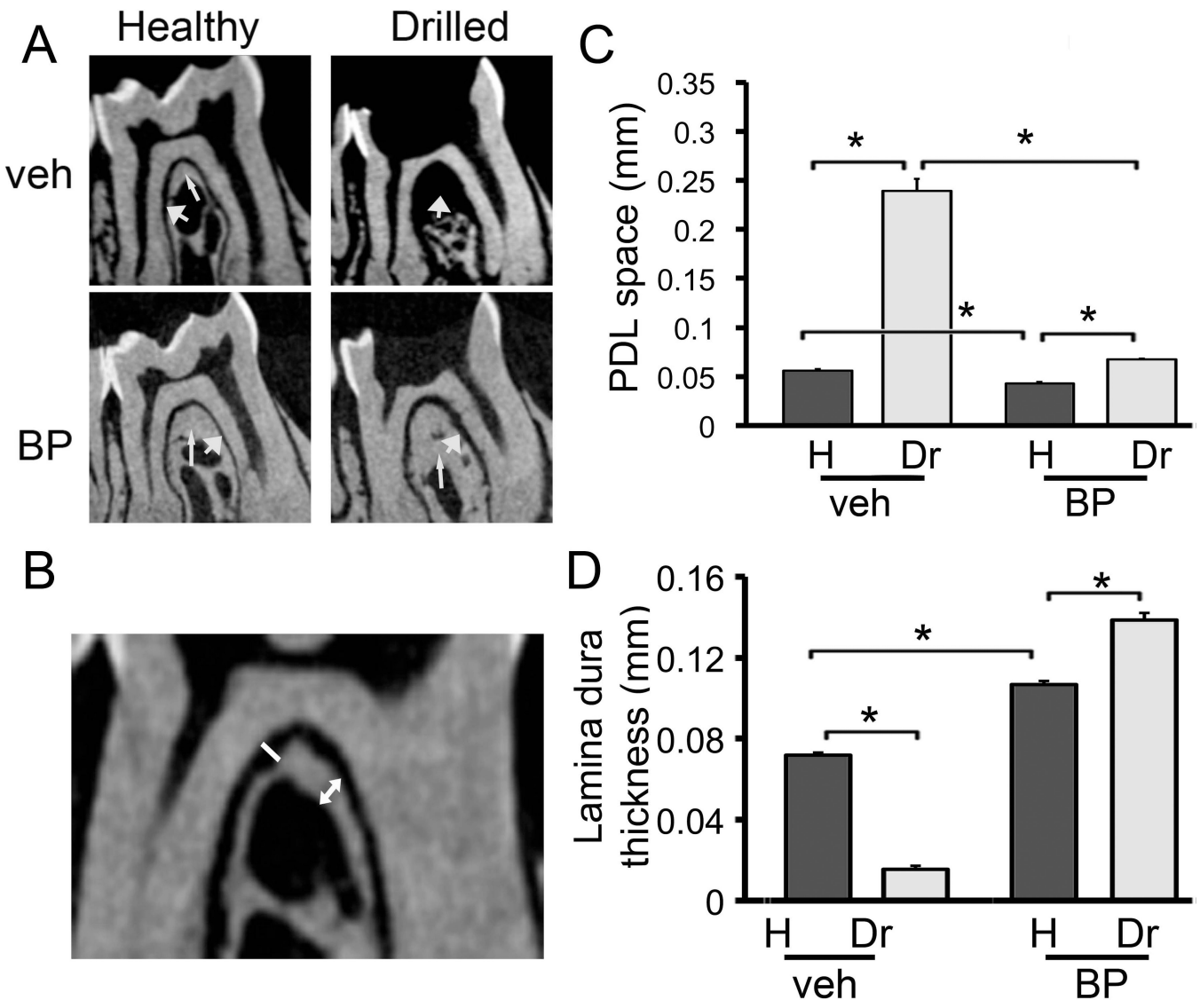

Figure 2.

Changes in the furcational periodontium of veh and BP treated animals. A) Representative μCT images of the furcation area of the first molar of healthy and drilled sites in veh or BP treated animals are shown. Thin arrow points to the lamina dura and thick arrow points to the PDL space. B) To quantify changes in the furcational periodontium, the width of the PDL space and the thickness of the lamina dura were measured at the furcation area. C) PDL space at the furcation area of the first molar. * statistically significantly different, $p<0.01$. D) Lamina dura thickness at the furcation area of the first molar. * statistically significantly different, $p<0.01$.

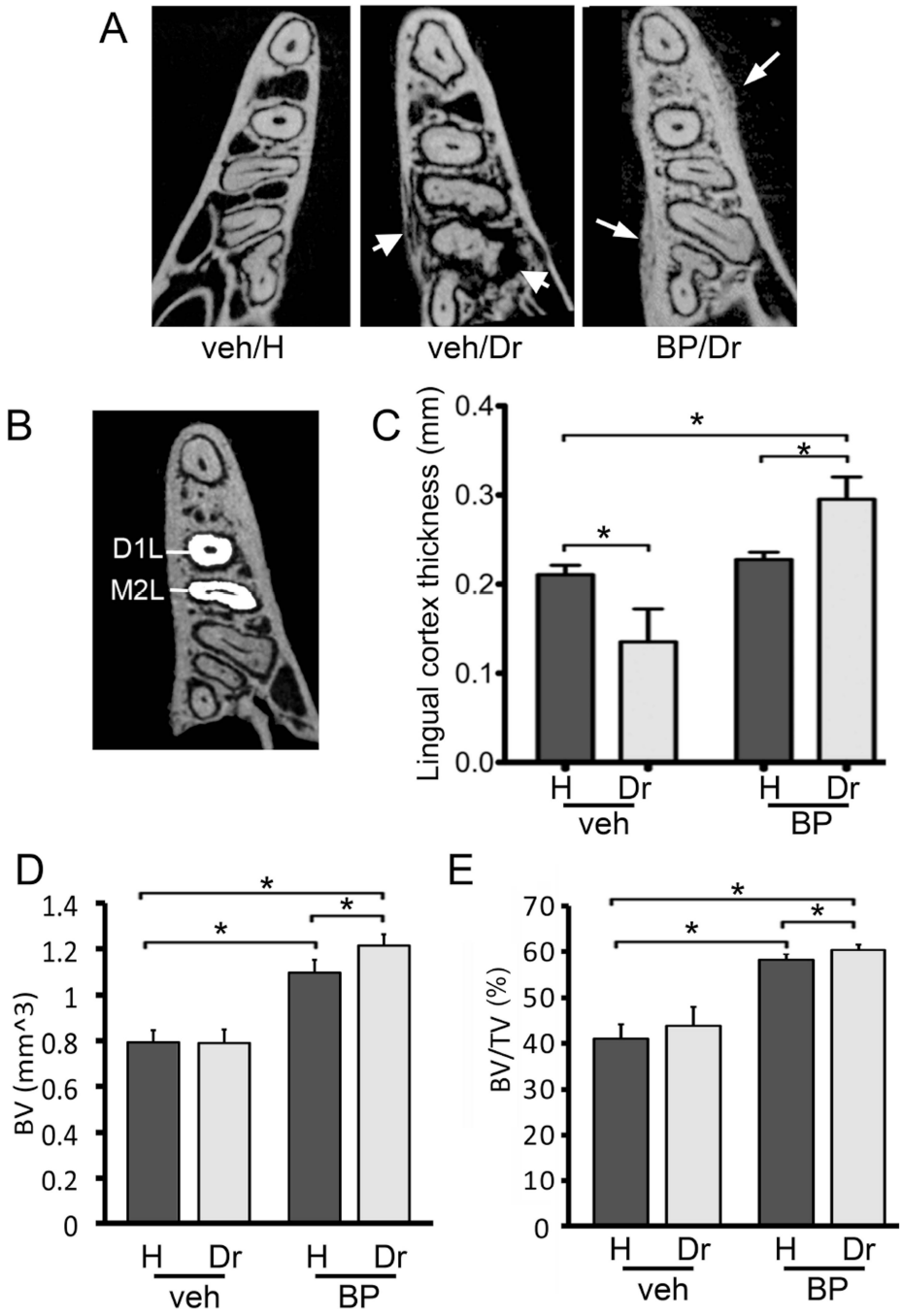

Figure 3.

Changes in alveolar bone structure in veh and BP treated animals. A) Representative axial μCT slices of the alveolar ridge at the apical third of the root are shown. Thick arrows point to osteolysis extending to the mandibular cortices seen in the drilled site of the veh treated animals. Thin arrows point to periosteal bone deposition and increased trabecular density seen in BP treated animals. B) To quantify the lingual bone thickness in veh vs. BP treated animals, the lingual width of the alveolar bone was measured at the distal root of the first moral and mesial root of the second molar in the healthy and drilled sites. C) Lingual cortex thickness at the distal root of the first molar. D) BV and E) BV/TV of bone at the area of the alveolar ridge. * statistically significantly different, $p<0.05$.

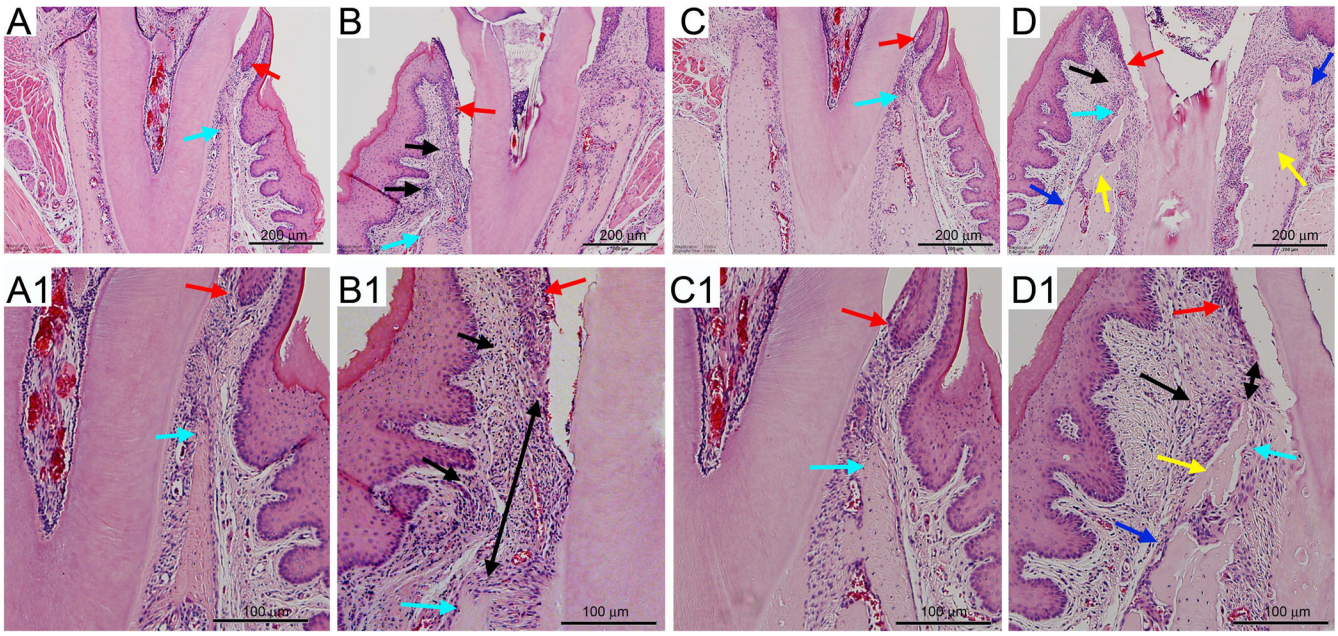

Figure 4.

Histologic examination of periodontal area of the alveolar bone. A, A1) Healthy site of a veh treated animal. B, B1) Drilled site of a veh treated animal. C, C1) Healthy site of a BP treated animal. D, D1) Drilled site of a BP treated animal. A, B, C, D are at 4X magnification, while A1, B1, C1, and D1 demonstrate a magnified area of A, B, C, and D. Red arrows point to marginal gingival epithelium, aqua to the crestal alveolar bone, black arrows to inflammatory infiltrate, black double arrows to the epithelial-crestal bone distance, yellow arrows to necrotic bone, and blue arrows to periosteal bone deposition.

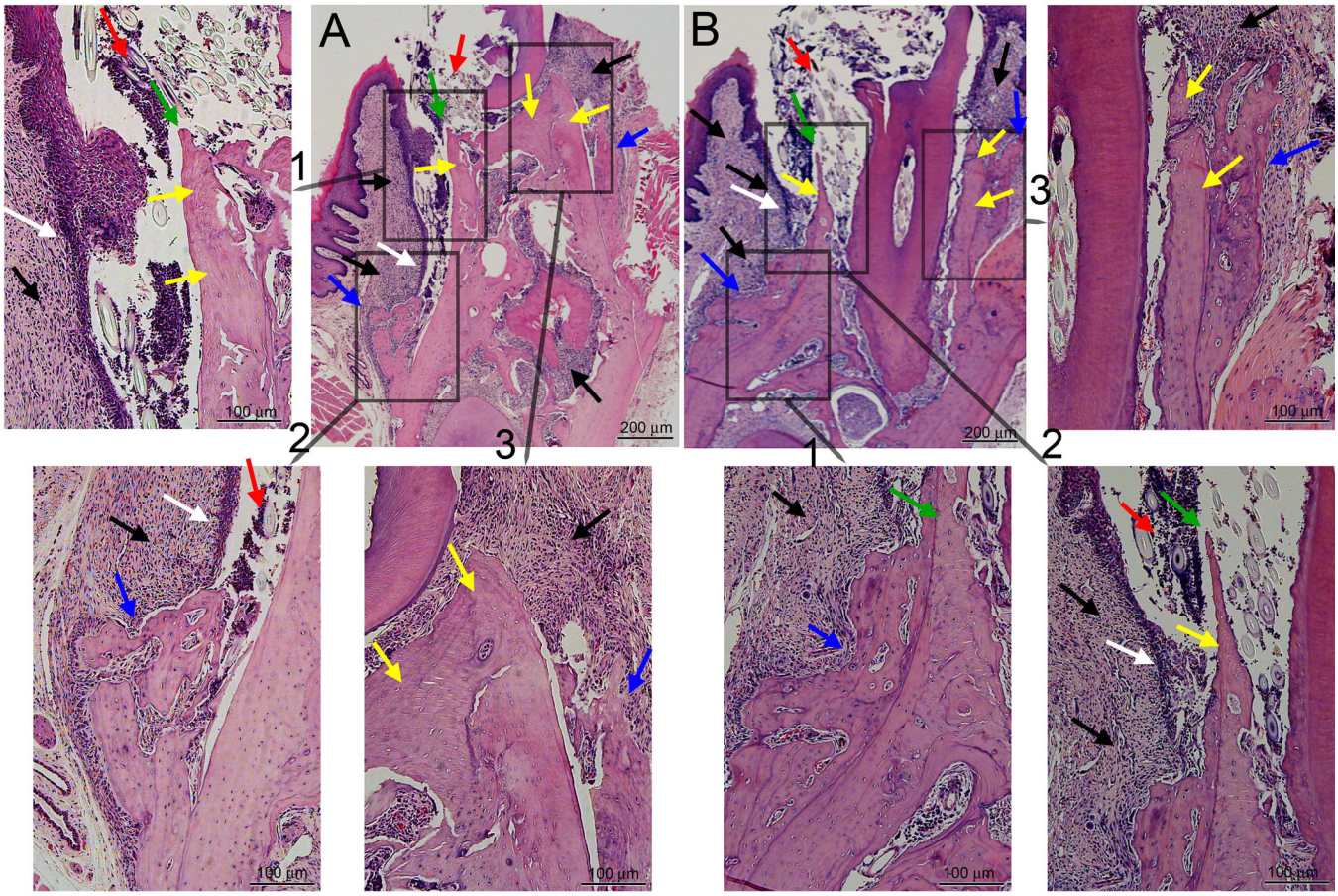

Figure 5.
Histologic examination of the drilled site of two BP treated animals (A and B) with bone exposure. A and B are at 4X magnification, while insets demonstrate magnified areas of A and B. Black arrows point to inflammatory infiltrate, white arrows to epithelial migration, yellow arrows to necrotic bone, green arrows to exposed bone, red arrows to debris, and blue arrows to periosteal bone deposition.

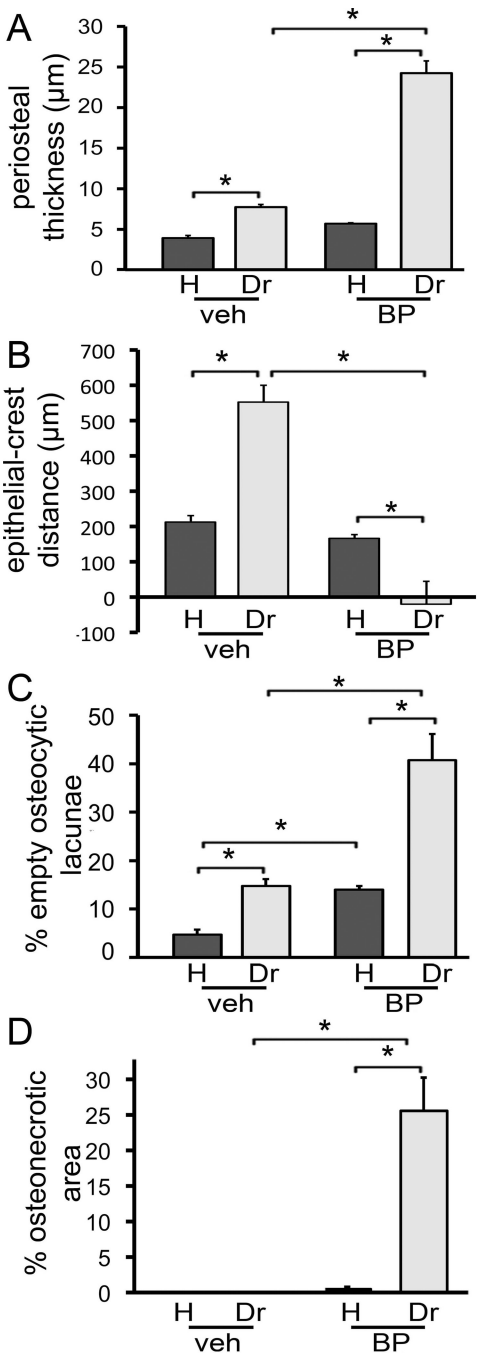

Figure 6.

Quantification of histologic findings. A) Thickness of periosteum at the buccal and lingual alveolus was measured. B) The shortest epithelial-crest distance was determined. If epithelium extended below the level of the alveolar crest, a negative value was assigned to the measurement. C) Osteocytic lacunae were measured and empty lacunae were expressed as percent of total. D) Area of osteonecrosis was measured and expressed as % of total bone area. * statistically significantly different, $p<0.01$.

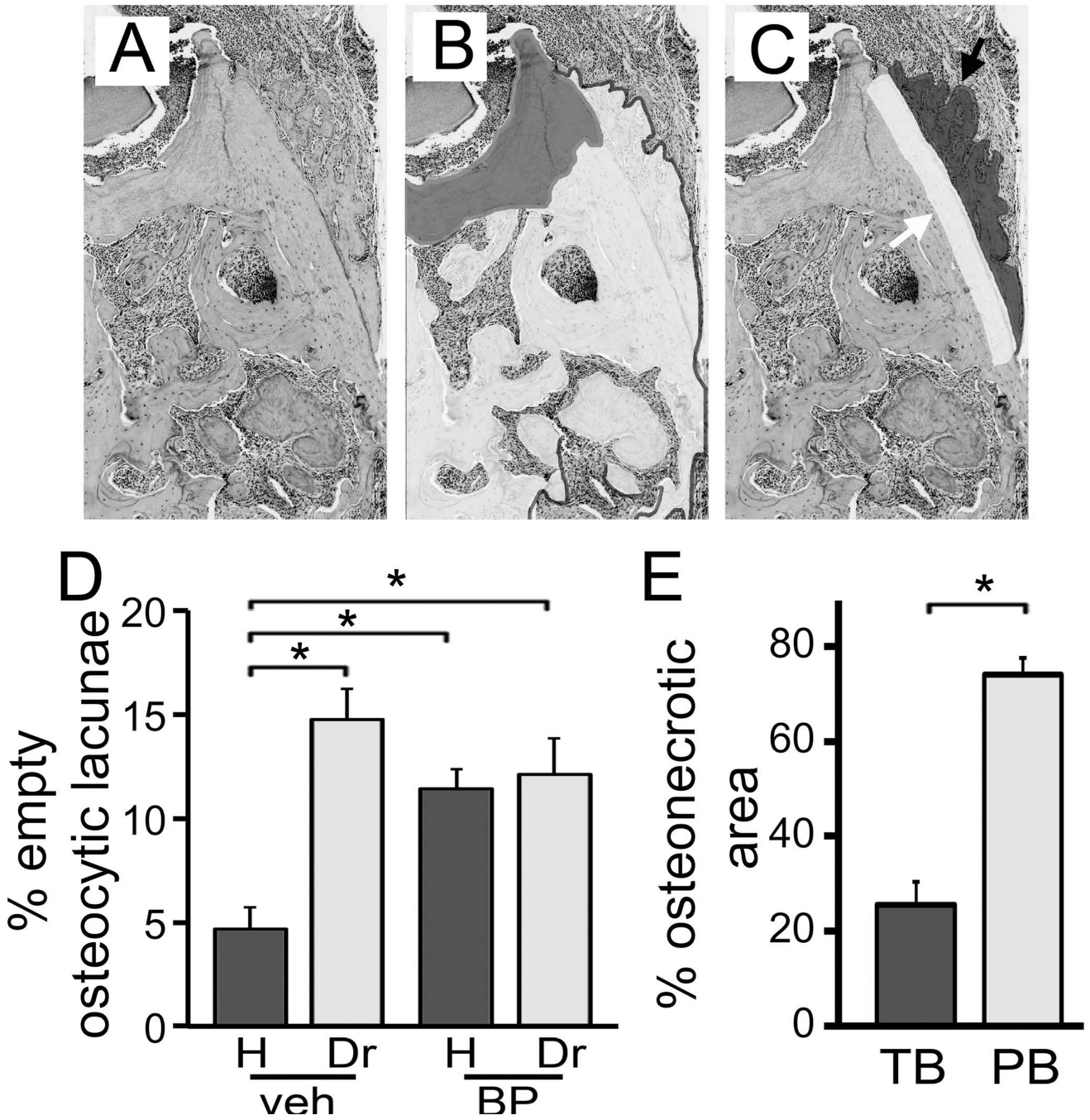

Figure 7.

Quantification of BP effects on empty osteocytic lacunae and osteonecrosis. A) Baseline histologic appearance of the area of interest. B) The necrotic (artificially shaded dark grey) and viable (artificially shaded white) bone areas were identified. C) The periosteal bone deposition (artificially shaded dark grey and black arrow) and adjacent 50 μm wide (artificially shaded white and white arrow) bone area were established. D) Osteocytic lacunae were measured in the areas of viable bone and empty lacunae were expressed as percent of total. E) The total bone % osteonecrotic area (TB) and % osteonecrotic area in a 50 μm wide band adjacent to periosteal bone (PB) were measured. * statistically significantly different, $p<0.01$.

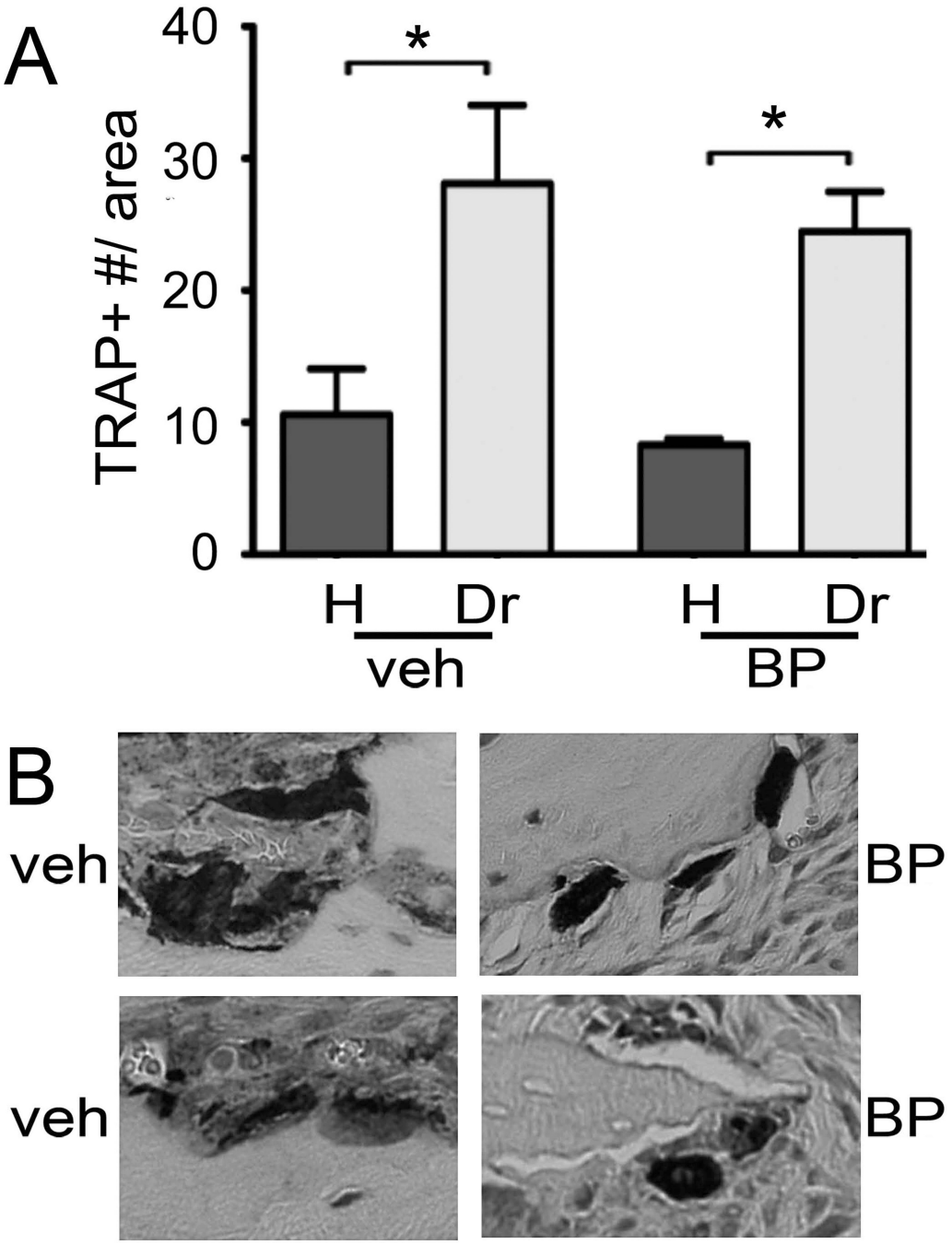

Figure 8.
Effects of BP treatment on TRAP+ cells. A) Number of TRAP+ cells in the healthy and drilled site of veh and BP treated animals. * statistically significantly different, $p<0.01$. B) Representative examples of TRAP+ cells from the drilled site of veh or BP treated animals.

TABLE 1

Radiographic and histologic findings in veh vs. BP treated animals

Treatment	Number of animals	Periosteal bone formation	Histologic Osteonecrosis	Bone Exposure
Veh	17	1 (6%)	0 (0%)	0 (0%)
ZA	18	17 (94%)	16 (88%)	6 (33%)